Article:
Harman-Thomas, J.M. orcid.org/0000-0003-3287-6050, Kashif, T.A., Hughes, K.J. orcid.org/0000-0002-5273-6998 et al. (2 more authors) (2023) Experimental and modelling study of syngas combustion in CO2 bath gas. Fuel, 342. 127865. ISSN: 0016-2361

https://doi.org/10.1016/j.fuel.2023.127865

Fuel 342 (2023) 127865

Contents lists available at ScienceDirect

Fuel

journal homepage: www.elsevier.com/locate/fuel

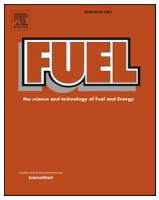

Full Length Article

Experimental and modelling study of syngas combustion in CO_2 bath gas

James M. Harman-Thomas [a,1], Touqeer Anwar Kashif [b,1], Kevin J. Hughes [a], Mohamed Pourkashanian [a], Aamir Farooq [b,*]

[a] The University of Sheffield, Department of Mechanical Engineering, Translational Energy Research Centre, Sheffield S9 1ZA, United Kingdom
[b] Clean Combustion Research Center, King Abdullah University of Science and Technology (KAUST), Thuwal 23955, Saudi Arabia

ARTICLE INFO

Keywords:
Supercritical CO_2
Syngas
Ignition delay time
Shock tube
Chemical kinetics

ABSTRACT

Syngas produced from coal and biomass gasification has been proposed as a potential fuel for direct-fired supercritical power cycles. For instance, the Allam-Fetvedt cycle can offer price-competitive electricity production with 100 % inherent carbon capture while utilizing CO_2 dilution of about 96 %. In this work, ignition delay times (IDTs) of syngas have been measured in CO_2 diluted conditions using a high-pressure shock tube at two pressures (20 and 40 bar) over a temperature range of 1100 – 1300 K. Syngas mixtures in this study were varied in equivalence ratio and H_2:CO ratios. The datasets were compared against the predictions of AramcoMech 2.0 and the University of Sheffield supercritical CO_2 2.0 (UoS sCO_2 2.0) kinetic models. Quantitative comparative analysis showed that the UoS sCO_2 2.0 was superior in its ability to predict the experimental IDTs of syngas combustion. We found that the reaction of CO_2 and H to form CO and OH caused the separation of H_2 and CO ignition in two events, which increased the complexity of determining the IDTs. We investigated this phenomenon and proposed a method to determine simulated IDTs for an effective comparison against the experimental IDTs. The chemical kinetics of syngas combustion in a CO_2 and N_2 bath gas are contrasted by sensitivity and rate-of-production analyses. By altering the ratio of H_2 and CO as well as mixture equivalence ratio, this work provides vital IDT data in CO_2 bath gas for further development and validation of relevant kinetics mechanisms.

1. Introduction

Combustion is predicted to remain a key component of the world energy economy until 2050 and beyond [1]. Therefore, to meet the strict decarbonization targets by 2060 or earlier, set by numerous countries following the Paris Agreement [2] and COP26 [3], emissions-free methods of generating energy from fossil fuels are required. One proposed technology, which is rapidly becoming established, is the direct-fired combustion of fossil fuels in supercritical carbon dioxide (sCO_2).

The Allam-Fetvedt cycle can operate with either synthesis gas (syngas) or natural gas, high-purity oxygen, and a large dilution of sCO_2 up to 96 % [4]. The combustion chamber of the Allam-Fetvedt cycle operates at 300 bar and temperatures of over 1000 K [5]. The key advantage of direct-fired sCO_2 combustion is the potential to inherently capture 100 % of the carbon dioxide (CO_2) produced without increasing the cost of electricity relative to the existing fossil fuel power plants without carbon capture [4]. The price of energy has become increasingly important, particularly in 2022, with energy prices soaring globally due to the rising cost of gas, the variability of renewables, and unanticipated political events [6]. A schematic of the Allam-Fetvedt cycle which utilizes syngas as a fuel may be found in Allam et al. [7].

The University of Sheffield (UoS) sCO_2 2.0 Mech was developed to model the high-pressure combustion of methane, hydrogen, and syngas in large dilutions of CO_2, based on shock tube ignition delay time (IDT) data [8,9]. UoS sCO_2 1.0 was demonstrated [8] to model methane and hydrogen combustion in CO_2 over a range of equivalence ratios and pressures within the average experimental error of the shock tube data (20–25 %). However, in the same study, a significant discrepancy was seen between the simulated and experimental syngas IDT datasets. UoS sCO_2 2.0 was subsequently developed based on eight new H_2 IDT datasets [9], as only three H_2 IDT datasets from Shao et al. [10] were used to validate the original version of the mechanism. In a review of the existing literature, it was found that the IDT determination using sidewall or endwall measurements could result in significantly different IDTs at specific thermodynamic/mixture conditions [9]. However, endwall measurements were determined to be the most representative of

* Corresponding author.
E-mail address: aamir.farooq@kaust.edu.sa (A. Farooq).
[1] Both Authors Contributed Equally.

https://doi.org/10.1016/j.fuel.2023.127865
Received 11 December 2022; Received in revised form 1 February 2023; Accepted 14 February 2023
Available online 24 February 2023

the true ignition phenomenon as the endwall diagnostics are less likely to be impacted by regions of premature/non-ideal ignition. This is consistent with Karimi et al. [11] who preferentially used endwall emission for the determination of syngas IDT in CO_2 at high pressures. Detailed discussion on this topic may be found in the literature [9,12] and is briefly addressed in the current work.

Five studies have been published on the IDTs of syngas in CO_2 by Vasu et al. [13], Barak et al. [14–16] and Karimi et al. [11]. A total of 20 IDT datasets were reported over 0.8 to 213 bar, equivalence ratios ranging 0.33 to 2.0, various bath gas compositions, and H_2:CO ratios.

The current work is aimed at obtaining high-temperature syngas IDT data at 20 bar in CO_2 bath gas, as previous studies did not investigate syngas IDTs at this pressure. Furthermore, we studied equivalence ratios down to $\phi = 0.25$ which has not been explored previously, and varied H_2:CO ratio from 4:1 to 1:4 to investigate the effect of this ratio on the overall ignition process. In addition, we measured a dataset at 40 bar, for which Barak et al. [15] found a poor agreement with the existing chemical kinetic mechanisms. This mixture also enabled an investigation into the discrepancy between the sidewall and endwall measurements used for determining IDTs. The datasets measured here are compared against the predictions of UoS sCO_2 2.0 and AramcoMech 2.0 models to evaluate their performance for CO_2-diluted syngas IDTs.

2. Experimental details

IDTs of various syngas mixtures were measured using the high-pressure shock tube (HPST) facility at King Abdullah University of Science and Technology (KAUST). The HPST is constructed from stainless steel and is capable of withstanding pressures up to 300 bar. The driven section is 6.6 m long with a circular cross-sectional diameter of 101.6 mm. The driver section is modular with three sub-sections, each measuring 2.2 m. For this study, the driver length was fixed at 2.2 m as this length was enough to produce the desired test times. The HPST houses a double-diaphragm arrangement which enables better shock-to-shock repeatability. Further details of the facility may be found elsewhere [17–19]. Mixtures were prepared in a magnetically-stirred 20 L stainless steel mixing vessel. Research grade (99.999 %) gases (H_2, CO, O_2, CO_2, N_2) from Air Liquide were used and each mixture was left for at least 4 h before experiments to ensure homogeneity. The eight mixtures investigated are shown in Table 1 along with the average absolute error value (E, %) for the two investigated mechanisms.

Incident shock speed was measured by six PCB 113B26 piezoelectric pressure transducers (PZTs) placed axially along the last 3.6 m of the driven section. Rankine-Hugnoit shock relations were utilized to calculate thermodynamic conditions (P_5 and T_5) behind reflected shock waves with uncertainties of <1 %. Incident shock attenuation rates varied from 0.5 to 1.8 %. Sidewall pressure was monitored using a Kistler 603B1 PZT, placed 10.48 mm away from the endwall, and OH* chemiluminescence signals were measured at the endwall and sidewall through photomultiplier tubes (PMTs).

For time zero extraction, literature works preferred endwall pressure for CO_2 diluted mixtures due to the reduced error in determining time-zero caused by bifurcation on the sidewall pressure trace [11,20]. Due to the lack of an endwall pressure transducer in our facility, the sidewall pressure signal was utilized, and the bath gas composition was reduced to 40 % CO_2 for most of the studied mixtures to reduce the impact of bifurcation. Fig. 1 shows that the sidewall pressure trace used to determine time zero was not as susceptible to bifurcation as in previous studies aside from the slight overshoot in pressure after the arrival of the reflected shock which is typical of shock tube experiments [11,20]. Conventionally, the mid-point of the steep reflected shock jump is taken as time-zero. However, shock bifurcation takes place in reflected shock gases with high CO_2 concentration, which causes a stepped pressure rise, thereby complicating the mid-point determination and time zero assignment. Therefore, in this study, time zero is defined at the instant of the beginning of the reflected shock pressure rise, as shown in Fig. 1. Similar strategy was adopted in our previous work [9].

The onset of ignition is determined from the steepest rise in the chemiluminescence trace of endwall OH* emission. In the present experiments, an earlier rise of OH* sidewall emission was observed compared to the endwall emission. This observation is consistent with that of Karimi et al. [11] and Harman-Thomas et al. [9]. Karimi et al. [11] associated this behaviour with localized hotspots developed near the sidewall due to the interaction of the reflected shock wave with the boundary layer. These hotspots result in the formation of ignition kernels around the periphery of the shock tube. However, due to the higher specific heat of CO_2, these kernels remain suppressed until the mixture auto-ignites at the core. Pryor et al. [21] pointed out similar observations from imaging experiments, where the developed kernels did not

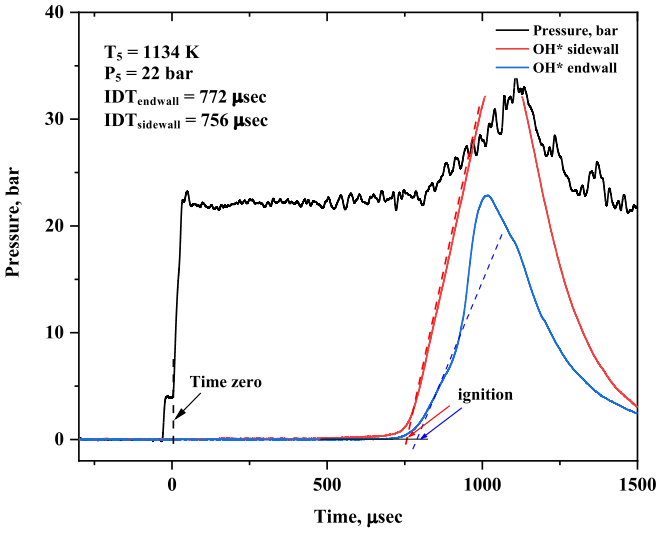

Fig. 1. Representative pressure (sidewall) and emission (sidewall, endwall) profiles for time zero and ignition determination from dataset 1.

Table 1
IDT mixtures studied in this work and quantitative comparison with the two mechanisms.

Mix.	Species Mole Fraction					Mixture Conditions				Average Absolute Error (E%)	
	H_2	CO	O_2	CO_2	N_2	T [K]	P [bar]	ϕ	θ	AramcoMech 2.0	UoS sCO_2 2.0
1	5	5	10	40	40	1135–1257	19.9–22.0	0.5	1.0	77.0	4.2
2	8	2	10	40	40	1102–1231	20.2–21.4	0.5	4.0	70.0	18.0
3	2	8	10	40	40	1155–1293	20.3–21.2	0.5	0.25	106.4	13.1
4	2.85	2.85	14.3	40	40	1142–1279	20.0–21.3	0.25	1.0	72.0	8.0
5	6.67	6.67	6.67	40	40	1127–1202	19.1–20.4	1.0	1.0	71.1	4.5
6	10.67	2.67	6.67	40	40	1139–1226	19.8–20.4	1.0	4.0	68.6	18.3
7	2.67	10.67	6.67	40	40	1135–1267	20.2–20.8	1.0	0.25	113.6	12.8
8	5	5	5	85	–	1145–1302	40.5–43.9	1.0	1.0	30.1	23.4
Average E (%)										76.1	12.9

θ = Mole fraction of H_2 divided by the mole fraction of CO.

affect the ignition of the core gas [21]. In this work, we diluted all mixtures but one in 40 % N_2 which further helped reduce the non-idealities arising from the polyatomic CO_2 bath gas.

3. Modelling procedure

A zero-D batch reactor with constant UV constraints in ANSYS Chemkin-Pro *R*3 (2019) was used to model IDTs with two chemical kinetic mechanisms, AramcoMech 2.0 [22] and UoS sCO_2 2.0 [9]. AramcoMech 2.0 is a comprehensive mechanism for the combustion of C1-C4 hydrocarbons and UoS sCO_2 2.0 was specifically developed to model the combustion of methane, hydrogen, and syngas in CO_2. The gradual increase in post-shock pressure (dp/dt) was accounted for by converting its experimentally determined average value to a pressure profile and incorporating that in Chemkin simulations. For the experiments reported here, values of dp/dt ranged 2–3 %/ms. The onset of ignition was defined as the time of the maximum gradient of the simulated OH time-history profile.

Normalized OH sensitivity analyses were used to identify the reactions which affected IDT predictions across the eight studied mixtures. A positive coefficient in the sensitivity analysis indicates that if a rate coefficient were to be increased, this would have a positive effect on OH concentration and thus decrease the IDT. A negative coefficient indicates the opposite in that increasing a rate coefficient will increase the IDT. These analyses were performed at the onset of ignition as simulated from the two mechanisms. In addition, the mechanism predictions were compared quantitatively using an average error between the simulated and experimental datapoints, as described previously [9].

3.1. Determining the simulated IDT of syngas

Simulations with AramcoMech 2.0 and UoS CO_2 2.0 revealed that some cases exhibited two peaks in the OH time history. The extent of the separation of the two peaks was dependent on the mixture composition and thermodynamic conditions, namely H_2:CO ratio, equivalence ratio, temperature, and pressure. Fig. 2 shows OH time-history profiles for dataset 3 (H_2:CO = 2:8) and dataset 4 (H_2:CO = 6.67:6.67) at 1188 K and 1169 K, respectively. The OH profile shows one distinct peak in Fig. 2 (a), whereas the profile is bimodal in Fig. 2 (b). At early times, the concentration of H_2 decreases faster since it is the more reactive fuel. In Fig. 2 (a), since the initial concentration of CO greatly exceeds that of H_2, the initial OH growth caused by H_2 oxidation gets subsumed by the OH formation from CO oxidation. However, in Fig. 2 (b), when both H_2 and CO amounts are equal, two distinct peaks in OH concentration are visible, and the gradient plot shows two clear points of maximum gradient corresponding to the two separate ignition events.

In instances where the two ignition events occur too close to be indistinguishable experimentally (~100 μs), an average of the two IDTs may be more illustrative of the experimental OH* chemiluminescence trail. Further complicating the process is the dominance of CO ignition when it is in surplus, as shown in Fig. 2 (a), where the second peak of OH due to CO ignition overshadows that of H_2. In this case, the second ignition may be used to represent the overall IDT since the first ignition event is undetectable experimentally. Therefore, depending on the conditions, the experimental IDT may be biased either toward the upper or lower bounds, or an average of both.

Fig. 3 shows experimental pressure as well as sidewall and endwall OH* chemiluminescence traces for dataset 1 (H_2:CO = 5:5) at 1145 K which shows a bimodal distribution in the sidewall OH* trace. Karimi et al. [11] also noted a bimodal peak in their OH* sidewall and endwall chemiluminescence traces, while studying the IDTs of syngas mixtures at pressures up to 100 bar. Bimodal ignition events are seen both in the simulations and in the experiments.

The bimodal ignition is further investigated by comparing the simulated OH mole fraction profiles in an 85 % CO_2 bath gas and an 85 % N_2 bath gas for dataset 8 (H_2:CO = 1). Fig. 4 (a) shows a bimodal and overall slower ignition, whereas Fig. 4 (b) shows almost simultaneous ignition events for H_2 and CO. This suggests that CO_2 has a chemical effect which slows down the oxidation of CO. Under these conditions,

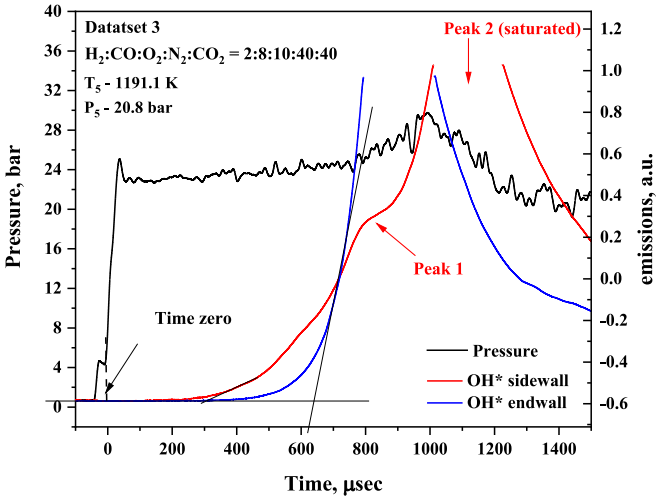

Fig. 3. Experimental pressure trace (left-hand axis) and OH* sidewall and endwall OH* emissions traces (right-hand axis) for Dataset 1 (H_2:CO:O_2:N_2:CO_2 = 5:5:10:40:40) at 1191 K and 20.8 bar.

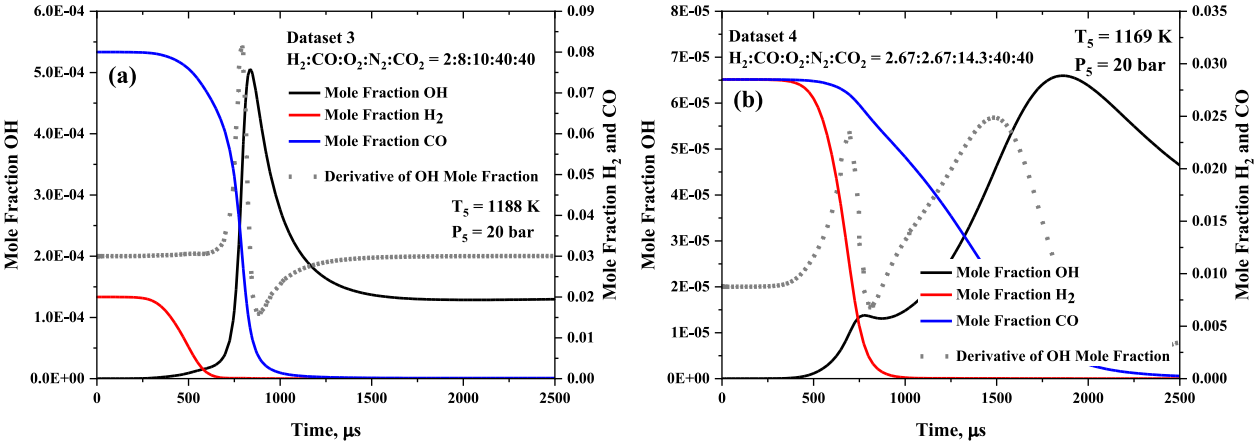

Fig. 2. Simulated mole fractions of OH, H_2 and CO for (a) Dataset 3 (H_2:CO:O_2:N_2:CO_2 = 2:8:10:40:40) and (b) Dataset 4 (H_2:CO:O_2:N_2:CO_2 = 2.85:2.85:14.3:40:40), modelled by UoS sCO_2 2.0.

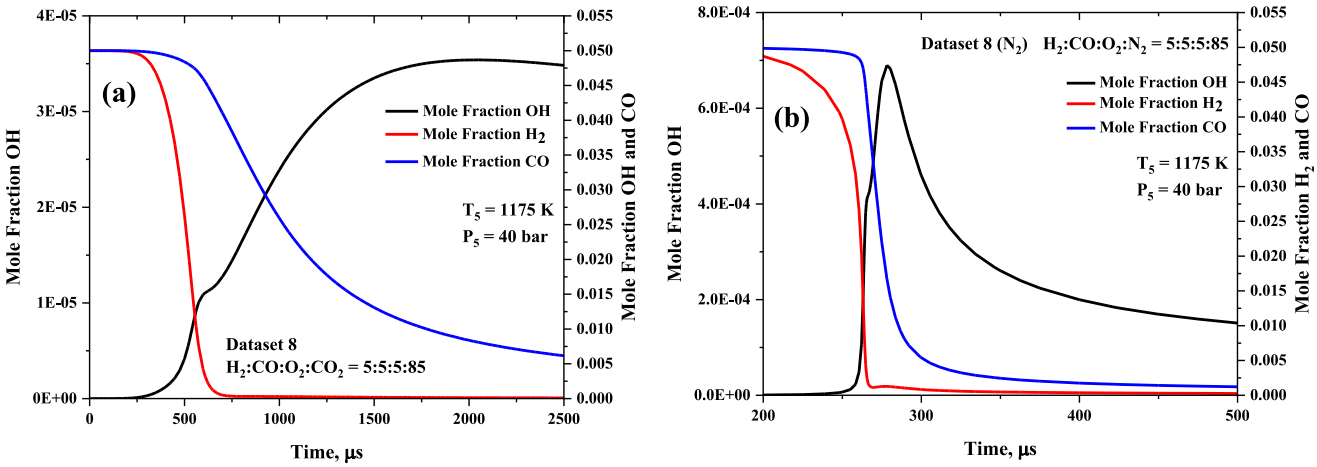

Fig. 4. Mole fraction of OH, H_2 and CO for (a) dataset 8 (H_2:CO:O_2:CO_2 = 5:5:5:85) and (b) dataset 8* (N_2) – (H_2:CO:O_2:N_2 = 5:5:5:85) modelled by UoS sCO_2 2.0.

almost all CO is consumed via Reaction 1 with all other reaction routes being negligible for both CO_2 and N_2 bath gas. At high concentrations of CO_2, the reverse of Reaction 1 reforms a significant amount of CO. Furthermore, the slower consumption of CO relative to H_2 is also because CO_2 bath gas reduces the maximum temperature achieved during combustion. This limits the rate of the temperature-dependant forward reaction, meaning that CO consumption occurs slower compared to N_2 bath gas. This can be shown via constant temperature simulations which indicate that CO consumption is significantly slowed relative to constant UV simulations (see Fig. S1). These two effects couple to reduce the overall rate of CO consumption via Reaction 1, meaning the two fuels get separated in two separate ignition events, making the determination of IDT more difficult.

Reaction 1. CO + OH ⇌ CO_2 + H

Therefore, when determining simulated IDTs in a CO_2 bath gas, and especially when studying syngas as a fuel where this effect is more pronounced, it is important to match the simulations to what is being observed experimentally. It is recommended to use the first ignition event in most instances as this will be the first peak observed experimentally. However, when CO is in a significant surplus in the syngas composition, the H_2 ignition event will likely be negligible on the experimental chemiluminescence trace, and it may be preferable to use the average IDT or the second ignition event, i.e., IDT of CO. For all works on syngas, the simulated and experimental IDT definitions must be clearly stated by the authors. In the current work, all simulated IDTs use the H_2 ignition event with the exceptions of datasets 3 and 7 (excess CO) where the average IDT of the two events is used. It is recommended that future works address this phenomenon further by using CO laser diagnostic to determine if simulations are correctly capturing the bimodal ignition. Whilst this observation is incredibly important to future works, it does not mean that existing IDT datasets are invalid; however, modellers should be careful when simulating IDTs of syngas in CO_2, especially when CO is in large excess.

4. Results and discussion

The discussion is split into four subsections, each analyzing the effect of a specific parameter on the measured and predicted IDTs. Table 1 lists the results of the quantitative comparison for AramcoMech 2.0 and UoS sCO_2 2.0 using the average percentage difference between the simulated and experimental runs across a given dataset, as described in Harman-Thomas et al. [9].

4.1. Effect of H_2:CO ratio at $\phi = 0.5$ and $\phi = 1.0$

The effect of altering the H_2:CO ratio (θ) at ϕ = 0.5 and ϕ = 1.0 is shown in Fig. 5 and Fig. 6, respectively. The experimental and simulated IDTs show that the mixture with the largest fraction of H_2 (dataset 2) shows the highest reactivity (shortest IDTs). Predictions of UoS sCO_2 2.0 are much better compared to AramcoMech 2.0. We can also observe quantitatively from Table 1 that UoS sCO_2 2.0 provides superior prediction for all six datasets. AramcoMech 2.0 consistently overpredicts IDTs, with the largest difference being at θ = 0.25. The best agreement between experiments and UoS sCO_2 2.0 is observed for θ = 1.0, and any deviation from this causes the mechanism to slightly overpredict measured IDTs. Fig. 6 also shows that the agreement is better for the stoichiometric mixture (ϕ = 1.0), consistent with the findings from Harman-Thomas et al. [9].

Sensitivity analyses were conducted to investigate the differences in syngas ignition for three different ratios of H_2:CO. It may be noted that most of the reactions featured in OH sensitivity in Fig. 7 are related to H_2 ignition, while CO ignition only features in two reactions. This is due to the two separate ignition events for H_2 and CO, as illustrated in Section

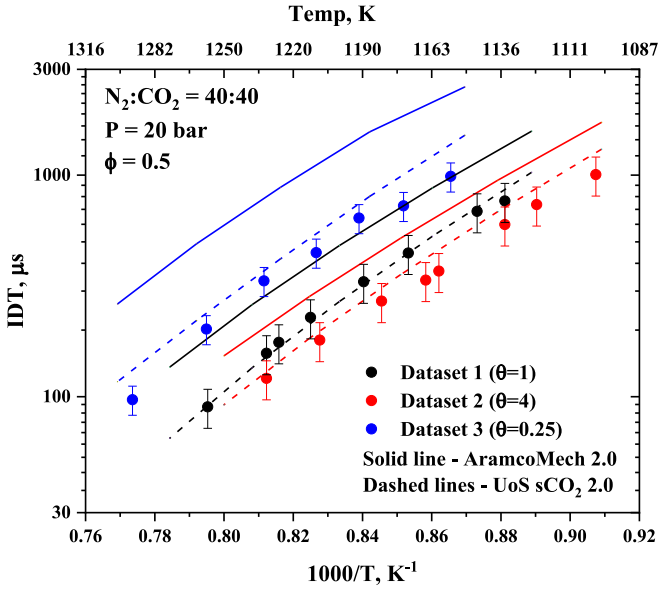

Fig. 5. Comparison of IDTs of datasets 1 (H_2:CO:O_2:N_2:CO_2 = 5:5:10:40:40), 2 (H_2:CO:O_2:N_2:CO_2 = 8:2:10:40:40) and 3 (H_2:CO:O_2:N_2:CO_2 = 2:8:10:40:40) with AramcoMech 2.0 and UoS sCO_2 2.0 simulations.

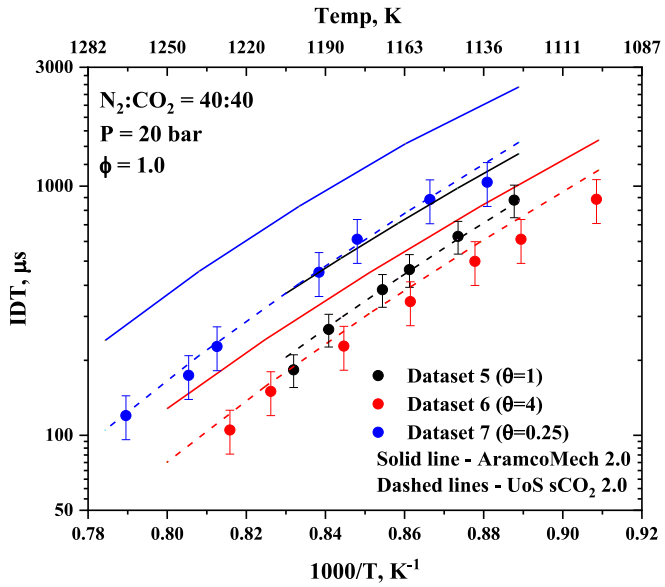

Fig. 6. Comparison of IDTs of datasets 5 (H_2:CO:O_2:N_2:CO_2 = 6.67:6.67:6.67:40:40), 6 (H_2:CO:O_2:N_2:CO_2 = 10.67:2.67:6.67:40:40) and 7 (H_2:CO:O_2:N_2:CO_2 = 2.67:10.67:6.67:40:40) with AramcoMech 2.0 and UoS sCO_2 2.0 simulations.

3.1. For dataset 2 (θ = 4.0) having excess H_2, the normalized OH sensitivity is very similar to that of dataset 1 (θ = 1.0), showing that the chemistry of H_2 is more important in determining the overall ignition due to the separation of the two peaks. For dataset 3 (θ = 0.25), a key difference is the smaller sensitivity toward H_2O_2 chemistry, particularly to Reaction 2 and Reaction 3, both responsible for consuming H_2O_2. This highlights the greater importance of H_2O_2 chemistry to datasets where CO is in excess (θ > 1.0). Rate-of-production (ROP) of HO_2 (Fig. S2) was investigated for dataset 3 to investigate why HO_2 becomes less important to the overall combustion mechanism when CO is in excess. ROP revealed that despite being a dominant reaction pathway at the point of H_2 ignition, Reaction 4 only accounts for a small amount of HO_2 loss during the ignition of CO. As discussed in Section 3, H_2 ignition is not quite detectable in the OH time history of dataset 3, meaning that it is the second (CO), larger ignition being defined as the overall IDT. This explains why H_2O_2 is not featured to be highly sensitive for dataset 3 (see Fig. 7).

Reaction 2. $H_2O_2 + H \rightleftharpoons HO_2 + H_2$

Reaction 3. $OH + OH\ (+M) \rightleftharpoons H_2O_2\ (+M)$

Reaction 4. $HO_2 + HO_2 \rightleftharpoons H_2O_2 + O_2$

Reaction 5. $H + O_2 \rightleftharpoons OH + O$

Reaction 6. $H + O_2\ (+M) \rightleftharpoons HO_2\ (+M)$

In Fig. 5, a better agreement of UoS sCO_2 2.0 with the experimental data was seen at higher temperatures and a slight overprediction at lower temperatures. To investigate this, normalized OH sensitivity analysis of dataset 2 (θ = 4.0) was performed at 1100 K and 1250 K (see Fig. 8). Although the fundamental reactions of H and O_2 show similar sensitivity, the main difference is in the sensitivity of reactions involving H_2O_2 (Reactions 2 and 3). This suggests that the chemistry of H_2O_2 is a key factor in the ignition of syngas at lower temperatures. Furthermore, ROP analysis shows that H_2O_2 is produced primarily through Reaction 4 and is consumed via the reverse of Reaction 3 (Fig. S3) to generate two OH radicals. At 1100 K, this pathway leads to about 76 % of OH production, and at 1250 K, it produces 36 % of total OH at the time of ignition.

In UoS sCO_2 2.0, the rate coefficient of Reaction 3 was taken from laser flash-photolysis measurements of Zellner et al. [23]. These measurements were made in an N_2 bath gas at a temperature and pressure of 353 K and 1100 mbar, respectively. The extrapolation of this rate coefficient to CO_2 bath gas, high temperatures, and high pressures may explain why UoS sCO_2 2.0 struggles to model the temperature dependence of some of the datasets. Although AramcoMech 2.0 uses a more recent theoretical rate coefficient of Reaction 3 from Troe et al. [24] in CO_2 bath gas, its overall prediction is significantly worse for the various syngas datasets. Therefore, the rate coefficient of Reaction 3 should be reinvestigated experimentally in CO_2 bath gas at higher pressures due to its importance in determining the temperature dependence of syngas IDTs at high pressures.

In the present work, AramcoMech 2.0 does not accurately predict syngas combustion with *E* (error) values as high as 81 %; a similar conclusion was seen in our previous work [8]. This inferior performance of AramcoMech is investigated using a normalized OH sensitivity analysis of dataset 5 (H_2:CO = 6.67:6.67). This dataset showed the best

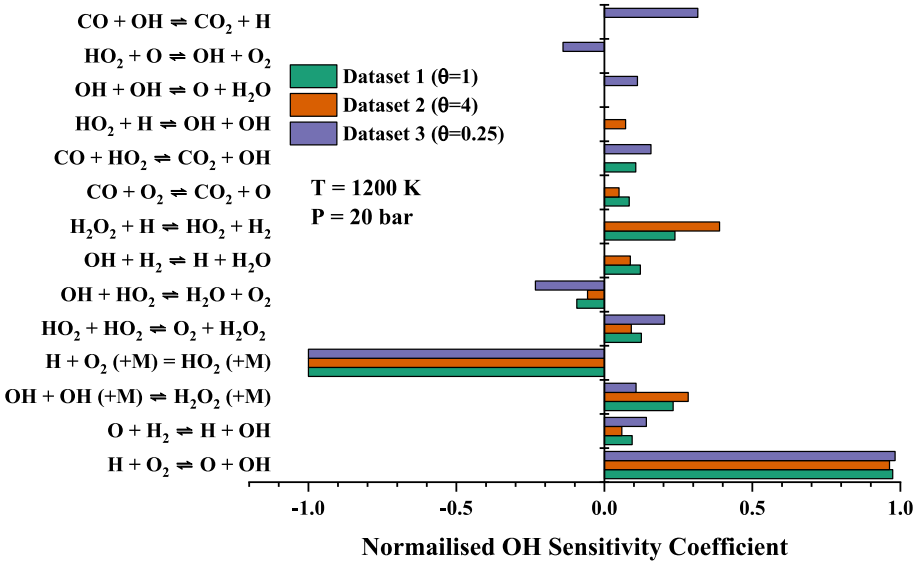

Fig. 7. Normalized OH sensitivity analyses for dataset 1 (H_2:CO:O_2:N_2:CO_2 = 5:5:10:40:40), 2 (H_2:CO:O_2:N_2:CO_2 = 8:2:10:40:40) and 3 (H_2:CO:O_2:N_2:CO_2 = 2:8:10:40:40) using UoS sCO_2 2.0.

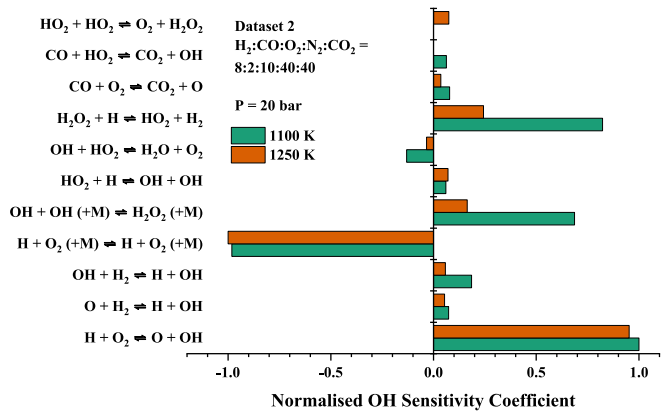

Fig. 8. Normalized OH sensitivity analysis of dataset 2 (H_2:CO:O_2:N_2:CO_2 = 8:2:10:40:40) for UoS sCO_2 2.0 at 1100 K and 1250 K.

agreement between the two mechanisms and experimental data among all datasets. Sensitivity analyses in Fig. 9 show that the normalized sensitivity coefficients for the key reactions are similar, indicating that the rate coefficients used in AramcoMech 2.0 for these reactions contribute to the overprediction of IDTs. Reaction 6 is the only reaction with a significant negative sensitivity coefficient for both mechanisms where a slightly smaller rate coefficient is used in UoS sCO_2 2.0 [8] than AramcoMech 2.0 [25]. The rate coefficients of Reaction 3 and Reaction 5 in UoS sCO_2 2.0 from Zellner et al. [23] and Yu et al. [26], respectively, are older than those used in AramcoMech 2.0 [24,27]. However, the larger overprediction of IDTs by AramcoMech 2.0 indicates that the faster rate coefficients implemented in UoS sCO_2 2.0 are essential to correctly model syngas ignition in CO_2 bath gas.

Interestingly, AramcoMech 2.0 performed better for H_2 ignition [9] despite the differences in rate coefficient and CO third body efficiency between AramcoMech 2.0 [24] and UoS sCO_2 2.0 [26] for Reaction 3. If the third body efficiency of the forward reaction is higher, then more OH is consumed to form H_2O_2. This would reduce the rate of OH production and result in longer IDTs of syngas combustion but this would not affect H_2 combustion. As a result, syngas IDT datasets from Karimi et al. [11] fit better with AramcoMech 2.0 because the CO concentration is much smaller than H_2. The performance of AramcoMech 2.0 worsens as the mole fraction of CO increases in the initial mixture. Unlike UoS sCO_2 2.0, which has the lowest *E* value for θ = 1.0, AramcoMech 2.0 performs best at large concentrations of H_2 and is significantly worse in predicting dataset 3 (8 % CO) and 7 (10.67 % CO) having θ = 0.25.

4.2. *Effect of equivalence ratio with excess CO (θ = 0.25)*

Simulated IDTs of UoS sCO_2 2.0 match measured IDTs of dataset 7 at ϕ = 1.0 within the 15 % uncertainty of the shock tube measurements, while dataset 3 at ϕ = 0.5 had the highest *E* of the studied datasets at 20 bar. As the discrepancy between the simulated and experimental IDTs for datasets 3 and 7 is consistent across the investigated temperature range, a sensitivity analysis was performed at the mid-point temperature of 1200 K. Fig. 10 demonstrates the similarity in the normalized OH sensitivity coefficients of datasets 3 and 7. A notable aspect is the presence of reactions representative of the two peaks in the OH sensitivity analyses despite the existence of only one peak in the OH mole fraction profile for both conditions. These peaks were further apart for dataset 3 (ϕ = 0.5) than for dataset 7 (ϕ = 1.0). Fig. 11 shows the mole fractions of OH, H_2 and CO for datasets 3 and 7 at 1200 K over the first 1500 μs of the combustion reaction. Clearly, in this instance, a single peak in the OH mole fraction curve is seen which is likely due to the smaller concentration of H_2 relative to CO, indicating that the H_2 peak is masked by CO. Fig. 11 also shows that the ignition of H_2 roughly occurs

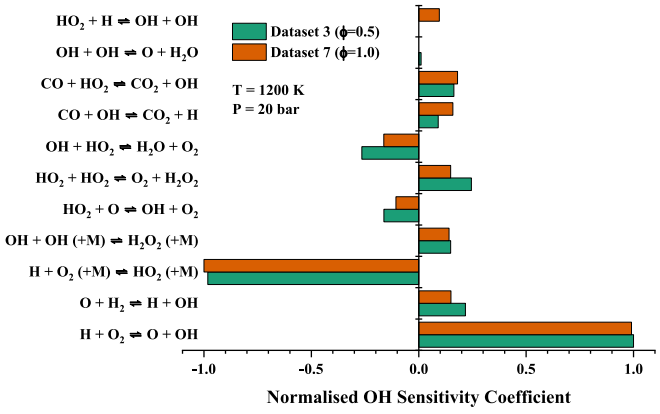

Fig. 10. Normalized OH sensitivity analyses of datasets 3 (H_2:CO:O_2:N_2:CO_2 = 2:8:10:40:40) and 7 (H_2:CO:O_2:N_2:CO_2 = 2.67:10.67:6.67:40:40) for UoS sCO_2 2.0 at 1200 K and 20 bar.

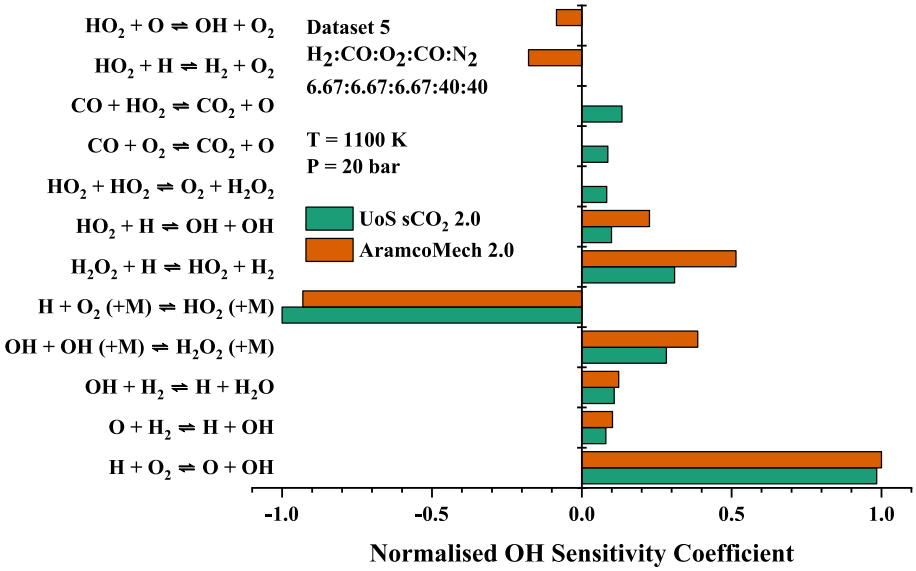

Fig. 9. Normalized OH sensitivity analysis of dataset 5 (H_2:CO:O_2:N_2:CO_2 = 6.67:6.67:6.67:40:40) for UoS sCO_2 2.0 and AramcoMech 2.0 at 1175 K and 20 bar.

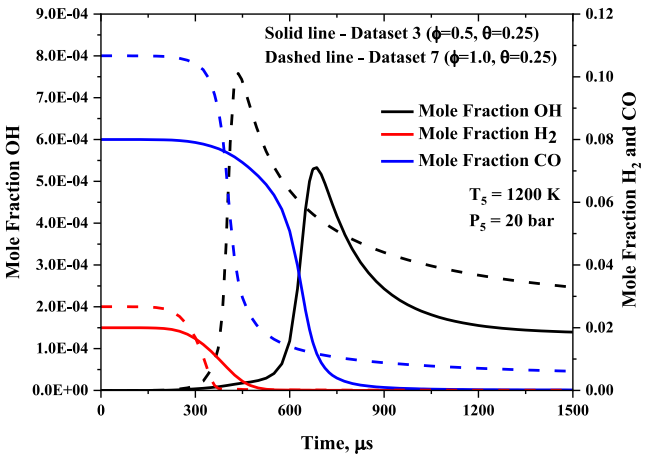

Fig. 11. Mole fraction of OH, H_2 and CO for datasets 3 ($\phi = 0.5$) and 7 ($\phi = 1.0$) at 20 bar and 1200 K.

between 300 and 450 μs for both datasets. However, for dataset 3 ($\phi = 0.5$), the subsequent ignition of CO occurs much later than for dataset 7 ($\phi = 1.0$), where the ignition of CO closely follows that of H_2. This affects the overall shape of the OH mole fraction curve, slowing the increase of OH which elongates the overall IDT.

4.3. *Effect of equivalence ratio for $\theta = 1.0$*

Fig. 12 shows the effect of altering the equivalence ratio ($\phi = 0.25$ to $\phi = 1.0$) at $\theta = 1.0$ for syngas combustion. Across the three datasets, UoS sCO_2 2.0 performs quite well, with each dataset having an *E* value of less than 10 %. AramcoMech 2.0 has a much larger *E* for the three datasets, though the overprediction is consistent across all three equivalence ratios.

Normalized OH sensitivity analyses of datasets 1, 4, and 5 reveal that the primary reactions of HO_2 have a similar OH sensitivity coefficient at all ϕ as shown in Fig. 13. For dataset 4 ($\phi = 0.25$), the dual peak of distinct H_2 and CO ignition is again observed as indicated by the sensitivity to both CO + OH and H + O_2 reactions. In these three datasets, the effect of changing the equivalence ratio is predicted more

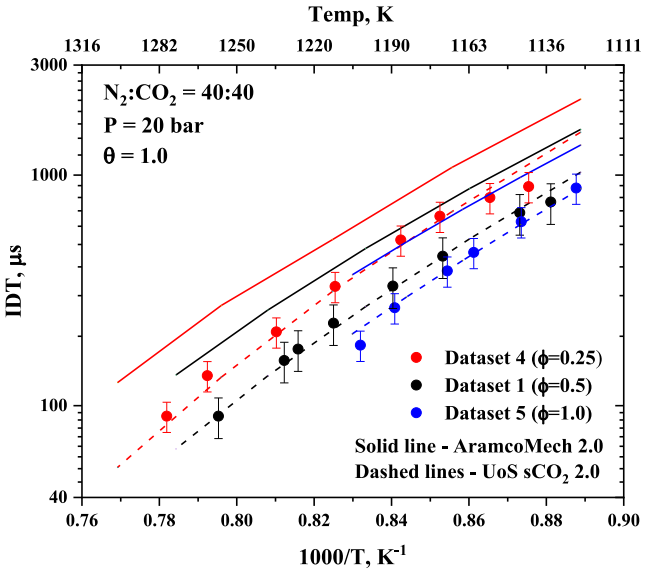

Fig. 12. Comparison of datasets 1 (H_2:CO:O_2:N_2:CO_2 = 5:5:10:40:40), 4 (H_2:CO:O_2:N_2:CO_2 = 2.85:2.85:14.3:40:40), and 5 (H_2:CO:O_2:N_2:CO_2 = 6.67:6.67:6.67:40:40) with AramcoMech 2.0 and UoS sCO_2 2.0.

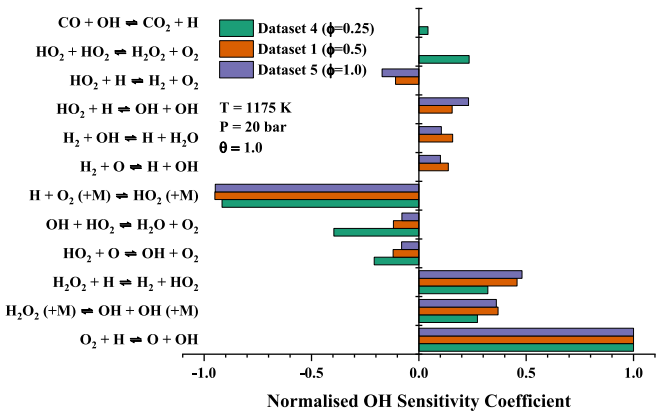

Fig. 13. Normalized OH sensitivity analysis of datasets 4 (H_2:CO:O_2:N_2:CO_2 = 2.85:2.85:14.3:40:40), 1 (H_2:CO:O_2:N_2:CO_2 = 5:5:10:40:40), and 5 (H_2:CO:O_2:N_2:CO_2 = 6.67:6.67:6.67:40:40) for UoS sCO_2 2.0 at 1175 K.

accurately, as shown by good IDT predictions in Fig. 12. This is consistent with *E* values in Table 1 which are consistently lower for the mixtures where $\theta = 1.0$. Nevertheless, for dataset 4, there is still a slight underprediction of IDTs at higher temperatures and an overprediction at lower temperatures, consistent with the discussion in Section 3.1. The mole fraction of OH, shown in Fig. 14. indicates that whilst both datasets 4 and 5 have two distinct OH peaks, dataset 4 ($\phi = 0.25$) peaks are much more separate than dataset 5 ($\phi = 1$).

Fig. 14 identifies different routes for OH production at $\phi = 0.25$ and $\phi = 1.0$ at the point of ignition. At $\phi = 0.25$, the majority of OH is produced via Reaction 3 (decomposition of H_2O_2). However, at $\phi = 1.0$, Reaction 3 plays a relatively small role in the production of OH while Reaction 5 and Reaction 7 become the key reactions for OH production. This can be explained by the smaller concentration of H radicals for $\phi = 0.25$ at the point of ignition. As revealed in the sensitivity analysis in Fig. 13, the two reactions of H and O_2, Reaction 5 and Reaction 6, are two of the most important reactions for syngas combustion in both datasets. Due to the greater concentration of O_2 in dataset 4, any H produced will react quickly via Reaction 5 or Reaction 6, and thus the radical pool of H atoms does not accumulate as quickly as it does for $\phi = 1.0$. This means that there are fewer H atoms available to react with HO_2 via Reaction 7, and thus this reaction pathway is less important for the formation of OH. Furthermore, Fig. 14 shows that both datasets have similar importance to Reaction 8, with it being the third largest contributor to OH formation at both conditions. Fig. 14 also shows that Reaction 9, a key contributor to OH production, peaks slightly later than the other reactions. This is due to the increasing concentration of H_2O as the reaction progresses.

Reaction 7. $HO_2 + H \rightleftharpoons OH + OH$

Reaction 8. $O + H_2 \rightleftharpoons H + OH$

Reaction 9. $OH + OH \rightleftharpoons O + H_2O$

The rate of loss of H atoms via three competing reactions, Reaction 5, Reaction 6, and Reaction 7, is plotted in Fig. 15. As expected, due to the abundance of O_2 at $\phi = 0.25$, Reaction 7 is a smaller pathway for the consumption of H atoms. Interestingly, the rate of Reaction 6 is much faster than Reaction 5 at $\phi = 0.25$ than it is at $\phi = 1.0$. This can be explained by the lower ignition temperature at $\phi = 0.25$. As temperature increases, the rate of the third body Reaction 6 decreases and the rate of Reaction 5 increases; thus at $\phi = 1.0$, the overall rate of loss of H atoms becomes similar. This effect is well captured by UoS sCO_2 2.0, which correctly predicts IDTs for all three equivalence ratios despite the chemistry of OH production varying as revealed by the sensitivity (Fig. 13) and ROP (Fig. 14) analyses.

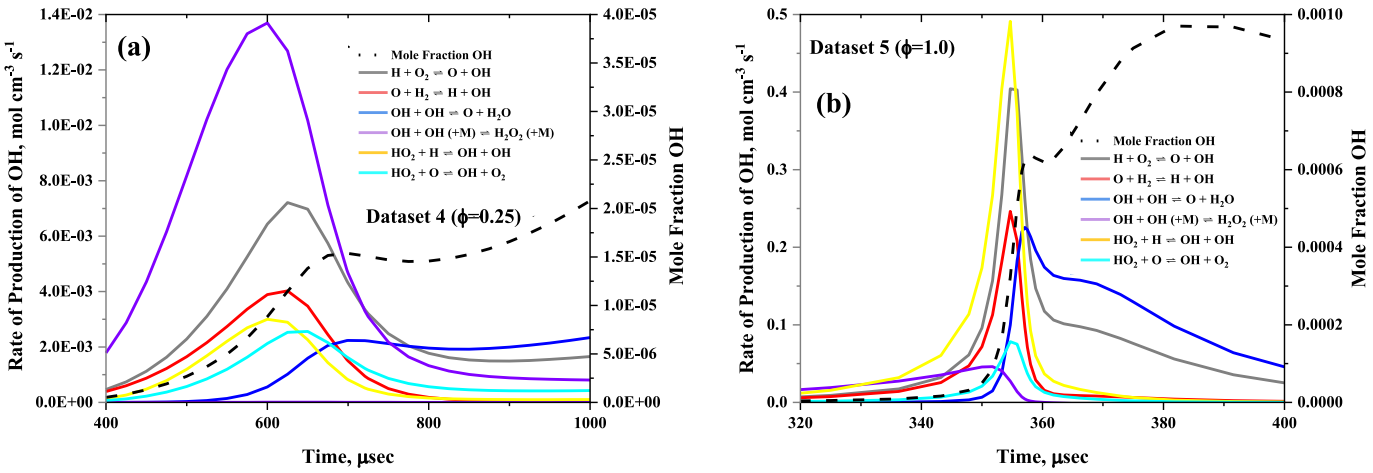

Fig. 14. Rate of production of OH and mole fraction of OH at 1175 K using UoS sCO_2 2.0 for (a) dataset 4 (ϕ = 0.25) and (b) dataset 5 (ϕ = 1.0).

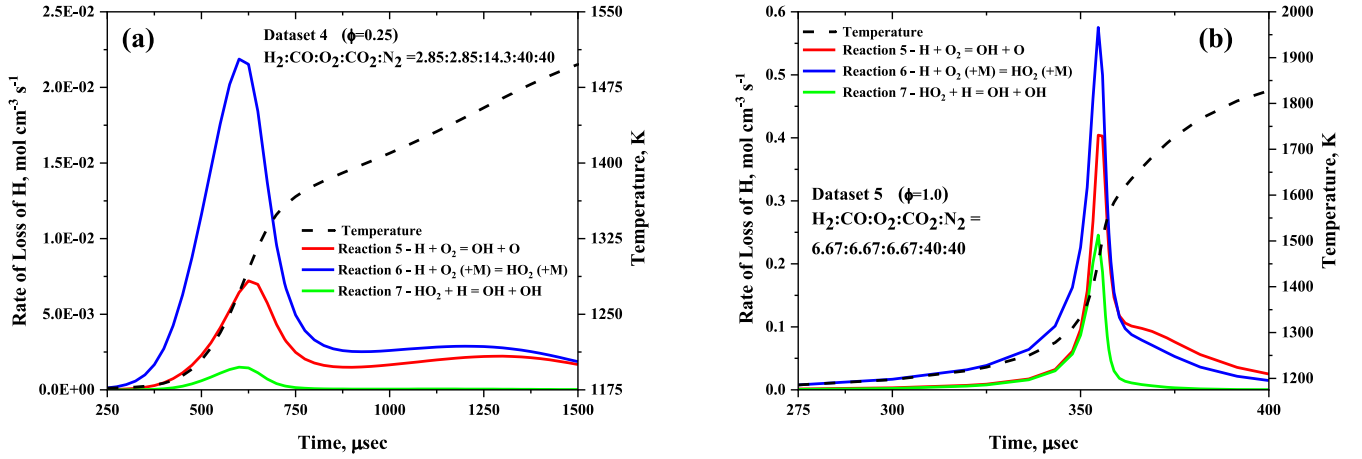

Fig. 15. Rate of loss of H atoms at 1175 K for (a) dataset 4 (ϕ = 0.25) and (b) dataset 5 (ϕ = 1.0).

4.4. *Comparison with Barak et al. [15] at 40 bar*

In addition to the seven datasets measured at 20 bar, a dataset was collected at 40 bar in 85 % dilution of CO_2 for a direct comparison with a dataset from Barak et al. [15]; this is shown in Fig. 16. In our work, IDTs were recorded using both sidewall and endwall OH* chemiluminescence. Our endwall measurements are longer than the sidewall, which is consistent with our previous work [9]. Harman-Thomas et al. [9] argued that endwall measurements are preferred for determining IDTs in CO_2 dilution due to the premature ignition being more pronounced in sidewall-mounted detectors. Despite some overlap with the sidewall measurements from the current work, IDTs from Barak et al. [15] are consistently faster. This is possibly due to the different effects of bifurcation in the two shock tubes or due to the different diagnostic technique used by Barak et al. [15] for IDT determination – sidewall emissions between 150 and 550 nm without any bandpass filter. Interestingly, Fig. 16 shows that AramcoMech 2.0 is in better agreement with dataset 8 (40 bar) than our datasets reported at 20 bar. The slight underprediction of UoS sCO_2 2.0 compared to the endwall measurements is likely an artefact of UoS sCO_2 being optimized using sidewall IDT measurements which are shown here to lead to an underprediction in the IDT, and could be improved in a future work by incorporating more endwall datasets.

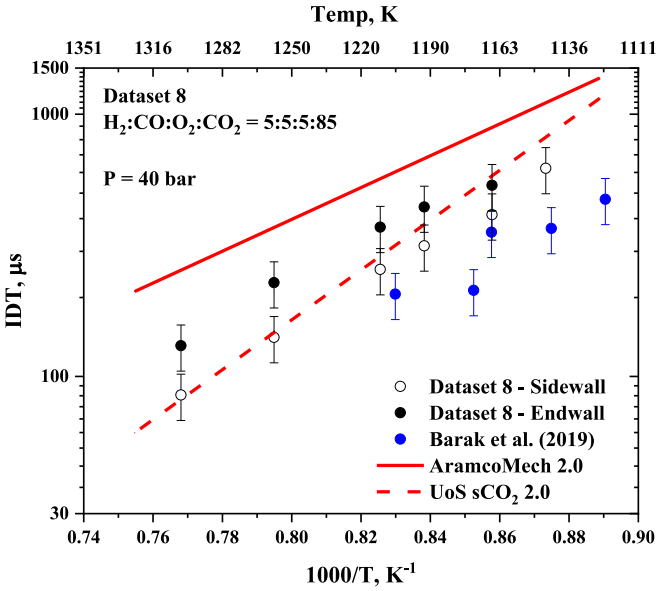

Fig. 16. Comparison of sidewall and endwall measurements of dataset 8 (H_2:CO:O_2:CO_2 = 5:5:5:85) with Barak et al. [15], and predictions of AramcoMech 2.0 and UoS sCO_2 2.0.

5. Conclusions

The combustion behaviour of various syngas mixtures diluted in CO_2 was investigated via IDT measurements at 20 and 40 bar over a range of equivalence ratios and H_2:CO ratios. This work focused on filling the gap in the literature for IDTs of syngas near 20 bar. The difficulty of defining IDT of syngas in CO_2 due to the separation of two distinct OH peaks was discussed and analyzed. Measured IDTs were used to validate UoS sCO_2 2.0 chemical kinetic mechanism and quantitative analysis showed it outperformed AramcoMech 2.0 across each of the eight investigated IDT datasets. Trends and discrepancies between the simulated and experimental IDTs were identified and explained using OH sensitivity and rate of production analyses. It was found that UoS sCO_2 2.0 could successfully predict syngas combustion at 20 bar over equivalence ratios of $\phi = 0.25–1.0$ but underperformed a bit as the H_2:CO ratio deviated from $\theta = 1.0$. The key reactions controlling syngas combustion were discussed and potential approaches to mechanism improvement were suggested, namely the chemistry of H_2O_2 and the reaction pathways of $H + O_2$ in CO_2 dilution. UoS sCO_2 2.0 has thus been successfully validated for its ability to adequately simulate the combustion of syngas in CO_2 across a variety of test gas compositions, temperatures, and pressures.

CRediT authorship contribution statement

James M. Harman-Thomas: Conceptualization, Methodology, Software, Formal analysis, Investigation, Writing – original draft, Visualization. **Touqeer Anwar Kashif:** Methodology, Software, Validation, Formal analysis, Investigation, Data curation, Writing – original draft. **Kevin J. Hughes:** Writing – review & editing, Supervision. **Mohamed Pourkashanian:** Supervision, Funding acquisition. **Aamir Farooq:** Writing – review & editing, Visualization, Supervision, Project administration, Funding acquisition.

Declaration of Competing Interest

The authors declare that they have no known competing financial interests or personal relationships that could have appeared to influence the work reported in this paper.

Data availability

IDT data is available as supplementary material and mechanisms are available in referenced publications.

Acknowledgements

The work of KAUST authors was funded by baseline research funds at King Abdullah University of Science and Technology (KAUST). This work has been supported by the EPSRC Centre for Doctoral Training in Resilient Decarbonised Fuel Energy Systems (Grant number: EP/S022996/1) and the International Flame Research Federation (IFRF).

Appendix A. Supplementary data

Supplementary data to this article can be found online at https://doi.org/10.1016/j.fuel.2023.127865.

References

[1] Welsby D, Price J, Pye S, Ekins P. Unextractable fossil fuels in a 1.5 °C world. Nature 2021;597(7875):230–4.
[2] Höhne N, Gidden MJ, den Elzen M, Hans F, Fyson C, Geiges A, et al. Wave of net zero emission targets opens window to meeting the Paris agreement. Nat Clim Change 2021.
[3] F.J. Kelly, COP26 – time for action, Air Quality, Atmosphere & Health 14 (2021) 1891-1891.
[4] Allam RJ, Palmer MR, Brown GW, Fetvedt J, Freed D, Nomoto H, et al. High efficiency and low cost of electricity generation from fossil fuels while eliminating atmospheric emissions, including carbon dioxide. GHGT-11 2013;37:1135–49.
[5] Allam RJ, Fetvedt JE, Forrest BA, Freed DA. The oxy-fuel, supercritical CO_2 Allam cycle: new cycle developments to produce even lower-cost electricity from fossil fuels without atmospheric emissions. Proceedings of the Asme Turbo Expo: Turbine Technical Conference and Exposition 3b. 2014.
[6] I. Liadze, C. Macchiarelli, P. Mortimer-Lee, P.S. Juanino, The Economic Costs of the Russia Ukraine Conflict, (2022).
[7] R. Allam, S. Martin, B. Forrest, J. Fetvedt, X.J. Lu, D. Freed, G.W. Brown, T. Sasaki, M. Itoh, J. Manning, Demonstration of the Allam Cycle: An update on the development status of a high efficiency supercritical carbon dioxide power process employing full carbon capture, 13th International Conference on Greenhouse Gas Control Technologies, Ghgt-13 114 (2017) 5948-5966.
[8] Harman-Thomas JM, Hughes KJ, Pourkashanian M. The development of a chemical kinetic mechanism for combustion in supercritical carbon dioxide. Energy 2022;255:124490.
[9] Harman-Thomas JM, Kashif TA, Hughes KJ, Pourkashanian M, Farooq A. Experimental and modelling study of hydrogen ignition in CO_2 bath gas. Fuel 2023;334:126664.
[10] Shao J, Choudhary R, Davidson DF, Hanson RK, Barak S, Vasu S. Ignition delay times of methane and hydrogen highly diluted in carbon dioxide at high pressures up to 300 atm. Proc Combust Inst 2019;37(4):4555–62.
[11] Karimi M, Ochs B, Sun W, Ranjan D. High pressure ignition delay times of H_2/CO mixture in carbon dioxide and argon diluent. Proc Combust Inst 2021;38(1):251–60.
[12] Karimi M, Ochs B, Liu ZF, Ranjan D, Sun WT. Measurement of methane autoignition delays in carbon dioxide and argon diluents at high pressure conditions. Combust Flame 2019;204:304–19.
[13] Vasu SS, Davidson DF, Hanson RK. Shock tube study of syngas ignition in rich CO_2 mixtures and determination of the rate of $H+O_2+ CO_2 \rightarrow HO_2+CO_2$. Energy Fuel 2011;25:990–7.
[14] Pryor O, Barak S, Koroglu B, Ninnemann E, Vasu SS. Measurements and interpretation of shock tube ignition delay times in highly CO_2 diluted mixtures using multiple diagnostics. Combust Flame 2017;180:63–76.
[15] Barak S, Ninnemann E, Neupane S, Barnes F, Kapat J, Vasu S. High-pressure oxy-syngas ignition delay times with CO_2 dilution: Shock tube measurements and comparison of the performance of kinetic mechanisms. J Eng Gas Turbines Power 2018;141.
[16] Barak S, Pryor O, Ninnemann E, Neupane S, Vasu S, Lu X, et al. Ignition delay times of oxy-syngas and oxy-methane in supercritical CO_2 mixtures for direct-fired cycles. J Eng Gas Turbines Power 2020;142.
[17] AlRamadan AS, Badra J, Javed T, Al-Abbad M, Bokhumseen N, Gaillard P, et al. Mixed butanols addition to gasoline surrogates: Shock tube ignition delay time measurements and chemical kinetic modeling. Combust Flame 2015;162:3971–9.
[18] AlAbbad M, Javed T, Khaled F, Badra J, Farooq A. Ignition delay time measurements of primary reference fuel blends. Combust Flame 2017;178:205–16.
[19] Alabbad M, Li Y, AlJohani K, Kenny G, Hakimov K, Al-lehaibi M, et al. Ignition delay time measurements of diesel and gasoline blends. Combust Flame 2020;222:460–75.
[20] Hargis JW, Petersen EL. Shock-Tube Boundary-Layer Effects on Reflected-Shock Conditions with and Without CO2. AIAA J 2017;55(3):902–12.
[21] Pryor O, Koroglu B, Barak S, Lopez J, Ninnemann E, Nash L, et al. Ignition delay times of high pressure oxy-methane combustion with high levels of CO_2 dilution, Proceedings of ASME Turbo Expo 2017: Turbo-machinery Technical Conference and Exposition. NC, USA: Charlotte; 2017.
[22] Metcalfe WK, Burke SM, Ahmed SS, Curran HJ. A hierarchical and comparative kinetic modeling study of C1–C2 hydrocarbon and oxygenated fuels. Int J Chem Kinet 2013;45:638–75.
[23] Zellner R, Ewig F, Paschke R, Wagner G. Pressure and temperature dependence of the gas-phase recombination of hydroxyl radicals. J Phys Chem 1988;92(14):4184–90.
[24] Troe J. The thermal dissociation/recombination reaction of hydrogen peroxide H_2O_2 (+M) ⇔ 2OH (+M) III.: Analysis and representation of the temperature and pressure dependence over wide ranges. Combust Flame 2011;158:594–601.
[25] Fernandes RX, Luther K, Troe J, Ushakov VG. Experimental and modelling study of the recombination reaction $H + O_2$ (+M) → HO_2 (+M) between 300 and 900 K, 1.5 and 950 bar, and in the bath gases M = He, Ar, and N_2. PCCP 2008;10:4313–21.
[26] Yu C-L, Frenklach M, Masten D, Hanson R, Bowman C. Reexamination of shock-tube measurements of the rate coefficient of $H+ O_2$ -> OH+ O. J Phys Chem 1994;98:4770–1.
[27] Hong Z, Davidson DF, Barbour EA, Hanson RK. A new shock tube study of the $H + O_2 \rightarrow OH + O$ reaction rate using tunable diode laser absorption of $_H2O$ near 2.5 μm. Proc Combust Inst 2011;33:309–16.